Mechanism and suppression of frictional chatter in high-efficiency elliptical vibration cutting

Hongjin Jung*, Takehiro Hayasaka, Eiji Shamoto (1)

Department of Mechanical Science and Engineering, Nagoya University, Furo-cho, Chikusa-ku, Nagoya, Aichi, 464-8603 Japan

This research clarifies the mechanism of undesirable vibration observed during high-efficiency elliptical vibration cutting. Elliptical vibration cutting has recently been utilized in practice, and some applications require high-efficiency machining at large width of cut causing vibration problems. Therefore, its mechanism is investigated by analyzing the finished surfaces and the undesirable vibrations superimposed on the elliptical vibration. The vibration is clarified as a kind of frictional chatter induced by ploughing on the tool flank at the beginning of cutting in elliptical vibration cycles and has unique characteristics such as occurrence with sharp tools, low amplitude, and surface waviness at beat frequency.

Chatter, Friction, Elliptical vibration cutting

1. Introduction

Since the introduction of the elliptical vibration cutting technology to the manufacturing field firstly in 1994, it has been demonstrated practically by many follow up studies that the technology has superior performance in diamond cutting of hardened die steel, i.e. high quality surface finish, long tool life and low cutting force compared to conventional cutting methods [1,2]. Meanwhile, with a recent industrial demand of low-cost mirror surface finishing of precision parts such as dies and molds, high-efficiency elliptical vibration cutting with a large width of cut has been proposed, and a high-power elliptical vibrator was developed which can generate the ultrasonic elliptical vibration against relatively large cutting load at a depth of cut of several hundred micrometers [3]. However, it sometimes causes an undesirable vibration problem. The vibration is small like a micrometer but should be suppressed for obtaining mirror surfaces and avoid wear and breakage of extremely sharp diamond tools.

Therefore, the generation mechanism of the undesirable vibration is investigated in this research by measuring and analyzing the finished surface profiles and the undesirable vibrations superimposed on the elliptical vibration. As a result, it is clarified that the undesirable vibration is a kind of frictional chatter [4,5,6] induced by the ploughing force acting on the tool flank only at the beginning of elliptical vibration cutting cycles. This mechanism leads to some unique characteristics such as occurrence with sharp cutting edges, low vibration amplitude, and cut surface waviness at the beat frequency between the elliptical vibration and chatter. Based on the clarified mechanism, a simple suppression method is also proposed, and its validity is verified experimentally.

2. Elliptical vibration cutting at large width of cut

2.1. Elliptical vibration cutting process and high-power device

In the elliptical vibration cutting process, the cutting edge vibrates mainly in two directions, i.e. cutting direction and depth of cut direction, with an elliptical locus as shown in Fig. 1(a). The cutting motion is applied relatively to the workpiece at the same time, so that it contacts the cut surface intermittently and pulls out the chip in each vibration cycle. Therefore, the cutting force is mainly caused by two processes, which are the ploughing process (shown mainly by A in Fig. 1(b)) and material removing process (shown mainly by B in Fig. 1(b)).

In order to realize the high-power elliptical vibration, relatively large piezoelectric actuators were utilized, which lead to low resonant frequency of 16.9 kHz. The 1st resonant mode of longitudinal vibration (depth of cut direction) and 3rd resonant mode of bending vibration (cutting direction) are excited in each direction as shown in Figs. 2(a) and 2(b) respectively [3]. This configuration is advantageous for practical usage, since the shape is similar to conventional tool shanks. However, the rod-shaped vibrator has bending vibration modes at lower resonant frequencies than its longitudinal modes, naturally. Hence, the developed vibrator has 1st and 2nd bending modes at lower frequencies than the elliptical vibration frequency, which may cause the undesirable vibration problem.

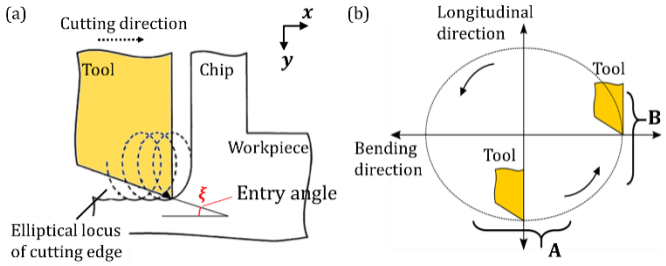

Figure 1. Elliptical vibration cutting process. (a) Schematic illustration of cutting process; (b) vibration locus of cutting edge.

2.2. Experimental setup and conditions

The experiments of elliptical vibration cutting at large width of cut were conducted on an ultra-precision machine tool (ASP01UPX, Nachi-Fujikoshi Corp.) equipped with the high-power elliptical vibration tool. Figure 3 shows a photograph of the experimental setup and a schematic illustration of the cutting process. The elliptical vibration tool is mounted on the B axis table, and the lead angle φ is set to be 0 deg, i.e. the vibrator axis is perpendicular to the finished surface. An inductive displacement sensor is used to measure the bending vibration of the elliptical vibration tool in the cutting direction. A typical hardened die steel (Stavax) was used as the workpiece. A single crystalline diamond tool with a nose radius of 1.0 mm was used to obtain mirror surfaces, and oil mist was supplied to the cutting point during the machining. A relatively large depth of cut d was set in a range from 0.1 mm to 0.3 mm, which leads to large width of cut as mirror-surface machining. Pick feed p was set to 0.020 mm for obtaining mirror surfaces with theoretical roughness of 0.05 μm. The experimental conditions are summarized in Table 1.

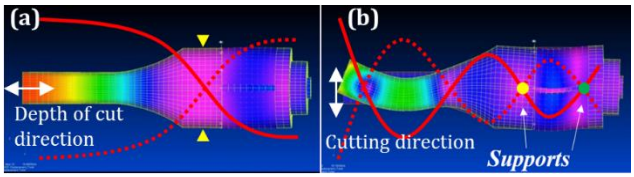

Figure 2. Vibration modes utilized for high-power ultrasonic elliptical vibration device [3]. (a) 1st mode of longitudinal vibration; (b) 3rd mode of bending vibration.

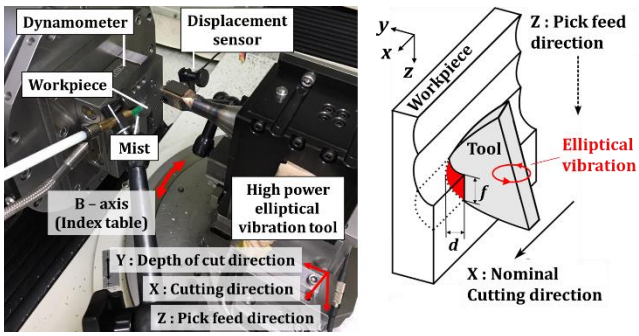

Figure 3. Photograph of experimental setup (Left) and schematic illustration of cutting process (Right).

Table 1
Experimental conditions

Workpiece	Material	Hardened die steel (ISO: 4028-400-00-I, Stavax)
	Hardness	53-54 HRC
Diamond tool	Nose radius (mm)	1.0
	Nominal rake angle (deg)	0
	Nominal clearance angle (deg)	10
Vibration conditions	Frequency f_1 (kHz)	16.9
	Amplitudes A_b, A_l (μm_{0-p})	5 (circular locus)
Cutting conditions	Lead angle φ (deg)	0
	Depth of cut d (mm)	0.1, 0.2, 0.3
	Pick feed p (mm)	0.020
	Cutting speed V_c (m/min)	1
	Cutting fluid	Oil mist

2.3. Experimental results

Figure 4 shows the FFT results of vibration measured in the bending direction during the machining. As shown in Fig. 4(a), there are large peaks around 16.9 kHz at all cutting conditions. This is the excited elliptical vibration which corresponds to the 3rd resonant mode of bending vibration. At large depths of cut d of 0.2 mm and 0.3 mm, undesirable vibrations, namely peaks at 10.71 kHz and 10.73 kHz respectively, were induced as shown in Fig. 4(b). Figure 4 (c) shows the short-time FFT results when depth of cut d=0.3 mm. The vibration grows and then peaks out from the middle of the machining. The undesirable vibrations at about 10.7 kHz correspond to the 2nd resonant mode of bending vibration of the vibrator.

This undesirable vibrations also affect the finished surfaces. Figure 5 shows a photograph of cut surfaces and the profiles of surfaces finished at different depths of cut. As observed in Fig. 5(a), mirror surfaces are obtained at all cutting conditions at the first glance. However, the surfaces finished at large depths of cut d =0.2, 0.3 mm are slightly cloudy due to the undesirable vibrations. As shown in Figs. 5(b), 5(c), and 5(d), the surface finished at d=0.1 mm is smooth and the feed marks are clearly observed, while the surfaces obtained at d=0.2, 0.3 mm are wavy along the cutting direction. The frequencies of the vibration marks can be calculated from the cutting speed and the wavelength, which is approximately around 6.2 kHz which corresponds to the beat frequency between the elliptical vibration and the undesirable vibration, and the amplitudes are less than about 0.1 μm_{p-p}.

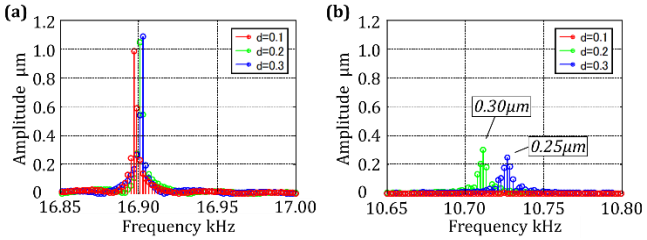

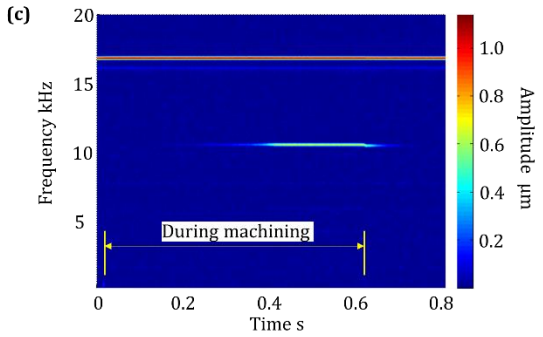

Figure 4. FFT results of bending vibration measured in cutting direction. (a) Frequency components from 16.85 kHz to 17.0 kHz (depth of cut: d=0.1, 0.2, 0.3 mm); (b) frequency components from 10.65 kHz to 10.8 kHz (depth of cut: d=0.1, 0.2, 0.3 mm); (c) time variation of frequency components (depth of cut: d=0.3 mm)

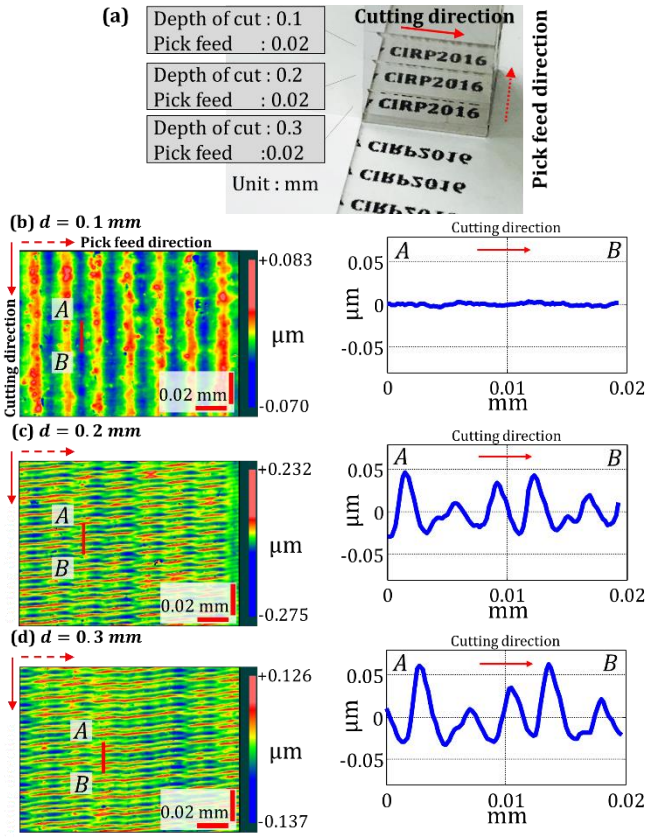

Figure 5. Photograph of machined mirror surfaces and surface profiles measured in cutting direction.

2.4. Analysis of cut surface from experimental results

To figure out the relationship between the induced vibration and the vibration marks on the cut surfaces, a time-domain simulations of the cutting edge locus during the machining are conducted according to the experimental results. Assuming that there is no vibration other than elliptical vibration, the cutting edge locus $L_1(x_1(t), y_1(t))$ can be expressed as follows.

$$x_1(t) = A_b \sin(2\pi f_1 t) + V_c t$$
$$y_1(t) = A_l \sin(2\pi f_1 t - \frac{\pi}{2}) \quad (1)$$

where x_1 and y_1 are the positions of the cutting edge in the cutting direction and the depth of cut direction respectively, A_b and A_l are vibration amplitudes in each direction, t is time, V_c is the cutting velocity, and f_1 is the frequency of elliptical vibration. Figure 6(a) shows the cutting edge locus $L_1(x_1(t), y_1(t))$ calculated under the same conditions as the experiments, see Table 1. As shown by the red line, the bottom parts of the locus remain as the cut surfaces, and its height or roughness is about 0.02 $\mu m_{p\text{-}p}$ and pitches are about 1 μm, which are equal in each elliptical cycle.

Next, the undesirable vibration induced at about 10.7 kHz at large depth of cut is also considered like as in the experimental results. Since there are no longitudinal modes around this frequency, the cutting edge would vibrate linearly in the 2nd bending mode. In addition, it is slightly inclined from the cutting direction because the position of the cutting edge is placed in front of the central axis of the bending vibration, as shown in Fig. 7(a). As a result, the cutting edge locus $L_2(x_2(t), y_2(t))$ can be expressed as follows.

$$x_2(t) = x_1(t) + A'_b \sin(2\pi f_2 t)$$
$$y_2(t) = y_1(t) + A'_b \sin(2\pi f_2 t) \tan(\theta) \quad (2)$$

Here, A'_b is the cutting-directional (horizontal) component of the 2nd resonant mode of bending vibration, f_2 is its frequency, and θ is the mode angle between the 2nd resonant mode of bending vibration and the cutting direction. θ was measured with a laser Doppler vibrometer, and its value is about 5 deg. The vibration amplitude during the machining was estimated by multiplying the measured vibration component at 10.73 kHz (0.5 μm, see Fig. 4(c)) and the mode ratio (× 2) measured preliminarily, i.e. $A'_b = 1$ μm. Other simulation conditions are the same as the above simulation without the undesirable vibration. Figure 6(b) shows the simulated cutting edge locus $L_2(x_2(t), y_2(t))$. As shown by the red line, the bottom parts remain as the cut surfaces and its amplitude is varied but in a range of smaller than about 0.1 $\mu m_{p\text{-}p}$ and the pitches also varied with a frequency of around 6.2 kHz. This simulation result agrees well with the experimental results shown in Fig. 5. Hence, it can be concluded that the 2nd resonant mode of bending causes the undesirable vibration during the machining with large width of cut, and the vibration marks are left at the beat frequency between the elliptical vibration and the undesirable vibration. Furthermore, Fig. 6(b) implies that the entry angle (see Fig. 1(a)) at the beginning of cutting in each elliptical vibration cycle varies significantly due to the undesirable vibration, i.e. the ploughing process shown by A in Fig. 1(b) varies significantly with the vibration.

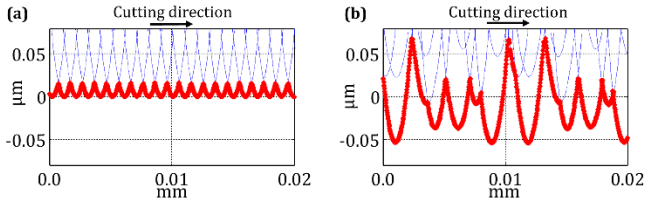

Figure 6. Simulated cutting edge loci. (a) Elliptical vibration; (b) elliptical vibration superimposed on 2nd resonant mode of bending vibration.

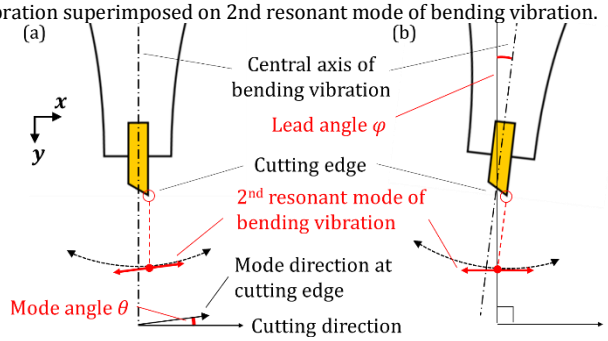

Figure 7. 2nd resonant mode of bending vibration of elliptical vibration tool and mode angle. (a) Upright posture which caused vibration problem; (b) tool posture with lead angle.

3. Discussion on mechanism of frictional chatter in elliptical vibration cutting process

From the above-mentioned time-domain simulation, the generation mechanism of the undesirable vibration can be explained as follows. In the elliptical vibration cutting, the ploughing process occurs only at the beginning of cutting in each elliptical vibration cycle. Thus, it is considered that the significant variation of entry angle can cause self-excitation force on the 2nd bending mode. Figure 8 shows schematic illustrations of the ploughing process just after the cutting edge enters the previously machined surface. Figure 8(a) shows the moment when the vibration speed in the 2nd bending mode (red arrow) becomes the minimum and the cutting speed (green arrow) is decreased and its direction becomes downward. Hence, the tool flank interferes more with the cut surface, and the frictional force F_e (thick red arrow) self-excites the vibration. On the other hand, Fig. 8(b) shows the ploughing process at the moment when the vibration speed (red arrow) becomes the maximum, i.e. the cutting speed (blue arrow) is increased and its direction becomes upward. Hence, the ploughing force acting on the tool flank is decreased, and its frictional component F_e (thick red arrow) is also decreased, i.e. F_e self-excites the vibration in this phase, too.

It should be noted that the regenerative effect also exists in this process, because the tool repeatedly cuts the surface machined in the previous elliptical vibration cycle. Hence, the cutting load and period in each cycle vary not only by the present undesirable vibration but also by the previous one left on the machined arc. This effect was also considered based on the time-domain simulation, but it is found that it generates damping force and cannot be a reason for the growth of the 2nd mode of bending vibration. For example, the shear force is constant in this cutting process because continuous chip is generated, and its thickness is constant [1,7]. Therefore, the time consumed for the material removing process of each elliptical vibration cycle is important, or in other words the absorbed energy during this process is roughly proportional to the length of the time. The material removing process starts when the cutting edge enters the previously machined surface (t_1 in Figs.8 (c), (d)). This time (t_1 in Figs.8 (c), (d)) is determined according to the previous elliptical vibration cycle and the present one in which the previous cycle can be considered as the regenerative effect. Then, the material removing process ends when the velocity in the

cutting direction becomes zero (t_2 in Figs.8 (c), (d)). When the vibration speed of the 2nd bending mode is minimum (Fig.8 (c)), the time consumed for the material removing process $t_2 - t_1$ becomes smaller than the one calculated for the maximum speed (Fig.8 (d)). Even if the previously cut surface regenerates in the worst phase meaning that the smallest t_1 for the minimum speed and the largest t_1 for the maximum speed, the time $t_2 - t_1$ becomes roughly the same for the both situations, i.e. the chatter is not either excited or damped by this effect, because the present cut is performed in the best phase to damp the chatter in any situation. This indicates that even if considering the worst case for the regenerative effect, it will not cause the chatter. Hence, it is considered that the frictional force in the ploughing process mainly acts as the self-excitation force due to the variation of the entry angle in each elliptical vibration cycle, which comes to the result that this undesirable vibration can be classified as a kind of frictional chatter.

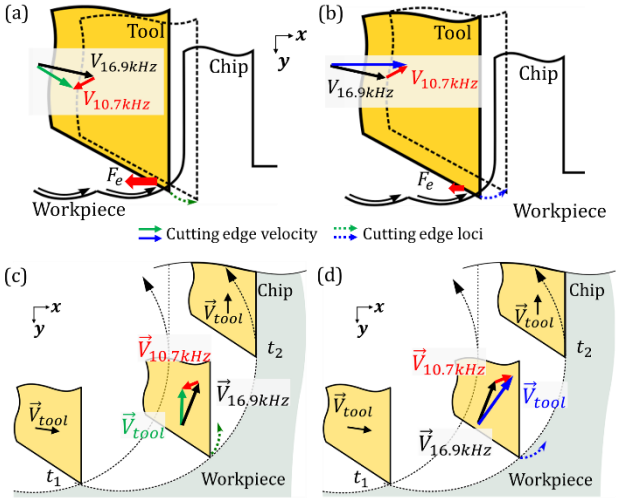

Figure 8. Ploughing process ((a),(b)) and material removing process ((c),(d)) in elliptical vibration cutting process, when cutting speed is (a),(c) decreased and (b),(d) increased by chatter vibration.

The mechanism should lead to some unique features of this chatter. The frictional chatter in the ordinary cutting does not occur with sharp cutting edges [4], while the chatter occurs in the elliptical vibration cutting with the single crystalline diamond tool which is extremely sharp. This is because the entry angle (as shown by ξ in Fig. 1(a)) can be large, e.g. entry angle ξ predicted theoretically under the conditions in Table 1 is 5.3 deg, which means that the tool burrows into the workpiece at the beginning of cutting in each elliptical vibration cycle. Moreover, not only the entry angle but the elastic deformation affects the contact between the tool flank and the workpiece, causing even more force to excite frictional chatter.

Another unique feature is the vibration amplitude. The frictional chatter usually grows up until the vibration speed reaches to the cutting speed [5,6], i.e. the amplitude becomes very large. On the other hand, the frictional chatter in the elliptical vibration cutting has a small amplitude (e.g. A'_b =1 μm as estimated in Section 2.4). This small amplitude can be explained by the small pitch of the vibration marks as follows. When the amplitude grows to be as large as the pitch, the entry angle variation changes because the number of vibration marks decreases and the entry height also varies considerably (Fig. 6(b)). The time-domain simulation shows that this effect of the height generates damping force by ploughing of past cutting marks, and thus the chatter vibration cannot grow to be very large in the elliptical vibration cutting.

4. Chatter suppression

Based on the generation mechanism, the frictional chatter in the elliptical vibration cutting should be affected by the lead angle of the vibration tool φ. For example, if the mode angle becomes zero by the lead, the instantaneous cutting direction (green and blue arrows in Fig. 8) does not change significantly. Thus, the chatter may be suppressed. Figure 7(b) shows the proposed method where the tool cuts the workpiece material with a lead angle φ of 5 deg which makes the mode angle to be 0 deg.

A series of experiments with the proposed method is conducted in order to investigate the validity against frictional chatter. The cutting conditions were kept the same with the previous experiments except that the lead angle φ is changed to be 5 deg by adjusting the B axis (see Fig. 3(left)).

Figure 9 (a) shows the FFT results of the vibration measured in the bending direction during the machining, and it can be confirmed that compared to Fig. 4(b) there are no peaks around the 2nd bending mode even at large depths of cut d of 0.2 and 0.3 mm. Figure 9 (b) shows the profile of surface finished at depth of cut d of 0.3 mm and it shows that there are no significant vibration marks along the cutting direction. These results verify the generation mechanism and that the proposed method is effective for suppressing frictional chatter, and elliptical vibration cutting can be performed at large widths of cut.

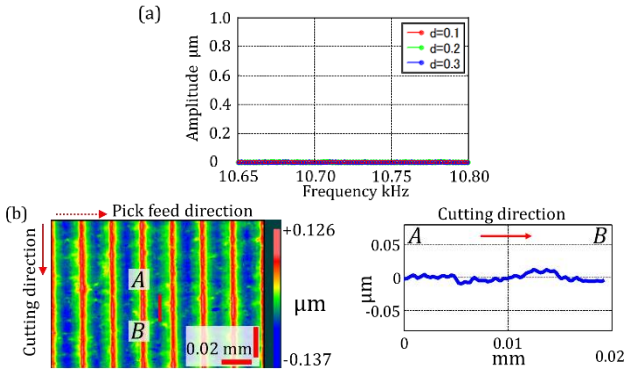

Figure 9. Machining results with lead angle for chatter suppression. (a) Frequency components of 10.65 kHz to 10.80 kHz of bending vibration measured during machining (depth of cut: d=0.1, 0.2, 0.3 mm); (b) surface profile along cutting direction (depth of cut: d=0.3 mm).

5. Conclusion

The mechanism of frictional chatter in elliptical vibration cutting was clarified in this study, i.e. it is self-excited by fluctuation of ploughing force acting on the tool flank at the beginning of cutting in elliptical vibration cycles. The mechanism leads to unique features such as occurrence with sharp tools, low amplitude and surface waviness at the beat frequency. Based on the mechanism, the lead angle of the vibration tool was improved, and it was clarified that the chatter can be suppressed successfully by the lead angle adjustment. As a result, the elliptical vibration cutting at large widths of cut was realized while clear mirror surfaces were obtained efficiently.

References

[1] Shamoto E, Moriwaki T (1994) Study on Elliptical Vibration Cutting. *Annals of the CIRP* 43(1): 35-38.

[2] Shamoto E, Moriwaki T (1999) Ultra-precision Diamond Cutting of Hardened Steel by Applying Elliptical Vibration Cutting. *Annals of the CIRP* 48(1): 441-444.

[3] Jung H, Shamoto E, Ueyama T, Hamada S, Xu Liangji (2016) Mirror Surface Finishing of Hardened Die Steel by High-Power Ultrasonic Elliptical Vibration Cutting. *Journal of Machining Engineering* 6(1): 5-14.

[4] Arnold R (1946) Cutting tools research: report of subcommittee on carbide tools: the mechanism of tool vibration in the cutting of steel. *Proceedings of the Institution of Mechanical Engineering* 154(1): 261-284.

[5] Wiercigroch M, Budak E (2001) Sources of nonlinearities: Chatter generation and suppression in metal cutting. *The Royal Society* 359(1781): 713-738.
[6] Altintas Y, Weck M (2004) Chatter Stability of Metal Cutting and Grinding. *Annals of the CIRP 53*(2):619-642
[7] Zhang X, Kumar A.S, Rahman M, Nath C, Liu K (2011) Experimental study on ultrasonic elliptical vibration cutting of hardened steel using PCD tools. *Journal of Materials Processing Technology* 211: 1701-1709.